^{1}H NMR Study of the Role of Heme Carboxylate Side Chains in Modulating Heme Pocket Structure and the Mechanism of Reconstitution of Cytochrome b_5†

Kang-Bong Lee, Gerd N. La Mar,* Ravindra K. Pandey, Irene N. Rezzano, Kathryn E. Mansfield, and Kevin M. Smith

Department of Chemistry, University of California, Davis, California 95616

Thomas C. Pochapsky‡ and Stephen G. Sligar

Department of Biochemistry, University of Illinois, Urbana, Illinois 61801

Received July 24, 1990; Revised Manuscript Received November 15, 1990

ABSTRACT: ^{1}H nuclear magnetic resonance spectroscopy was used to assign the hyperfine-shifted resonances and determine the position of a side chain in the heme cavity of wild-type rat apocytochrome b_5 reconstituted with a series of synthetic hemins possessing systematically perturbed carboxylate side chains. The hemins included protohemin derivatives with individually removed or pairwise shortened and lengthened carboxylate side chains, as well as (propionate)n(methyl)$_{8-n}$porphine–iron(III) isomers with n = 1–3 designed to force occupation of nonnative propionate sites. The resonance assignments were effected on the basis of available empirical heme contact shift correlations and steady-state nuclear Overhauser effect measurements in the low-spin oxidized proteins. The failure to detect holoproteins with certain hemins dictates that the stable holoproteins, unlike the case of myoglobin, demand the axial iron–His bonds and cannot accommodate carboxylate side chains at interior positions in the binding pocket. Hence, the heme pocket interior in cytochrome b_5 is judged much less polar and less sterically accommodating than that of myoglobin. The propionate occupational preference was greatest as the native 7-propionate site, but also possible at the nonnative crystallographic 5-methyl or 8-methyl positions. Only for a propionate at the crystallographic 8-methyl position was a signifiant perturbation of the native molecular/electronic structure observed, and this was attributed to an alternative propionate–protein hydrogen bond at the crystallographic 8-methyl position. The structures of the transient protein complexes detected only shortly after reconstitution reveal that the initial encounter complexes during assembly of holoprotein from apoprotein and hemin involve one of the two alternate propionate–protein links at either the 7-propionate or native 8-methyl position. In a monopropionate hemin, this leads to the characterization of a new type of heme orientational disorder involving rotation about a N–Fe–N axis.

Cytochrome b_5 is a *b*-type hemoprotein that serves as electron mediator in stearyl-CoA[1] desaturation (Strittmatter et al., 1974), cytochrome P-450 reductase (Tamburini & Schenkman, 1986), and methemoglobin reductase systems (Hultquist et al., 1984) in vivo. Because of the small size of the solubilized microsomal fragment, it has been the subject of intense study for the purpose of defining in detail the structural bases of the factors that control both redox potential (Reid et al., 1982, 1984, 1986; Walker et al., 1988; Funk et al., 1990) and the mechanism of electron transfer between pairs of complementary redox partner proteins (Salemme, 1976; Mauk et al., 1982; Mauk & Mauk, 1982; Livingston et al., 1985; McLachlan et al., 1986; Wendolosk et al., 1987). Various features of the unique binding of the heme to the apoprotein (Mathews et al., 1979), as well as the distribution of charged surface residues (Reid et al., 1984; Livingston et al., 1985), have been invoked to rationalize the relatively low redox potential exhibited by these *b*-type cytochromes. The carboxylate side chains of cytochrome b_5 have been implicated in two types of control of redox role. On the one hand, several surface Asp and Glu residues, as well as one heme propionate extended into solution, appear to serve as recognition sites for formation of well-defined 1:1 complexes via charge-complementary docking with the similarly situated positively charged residues on partner redox proteins (Salemme, 1976; Mauk et al., 1982; Mauk & Mauk, 1982; Livingston et al., 1985; McLachlan et al., 1986; Wendolosk et al., 1987). Such partner proteins include hemoglobin (Mauk & Mauk, 1982), myoglobin (Livingston et al., 1985), cytochrome P-450 (Stayton et al., 1988), and cytochrome *c* (Salemme, 1976; Mauk et al., 1982; Eley & Moore, 1983; Wendolosk et al., 1987; Rogers et al., 1988), and the stereospecificity of the docking interaction likely facilitates the electron transfer process. The second heme propionate, on the other hand, makes an important protein–heme link (Mathews et al., 1979) and has been proposed to modulate the heme redox potential by charge stabilizing the ferric ion (Mathews et al., 1979; Reid et al., 1984). Both of these control mechanisms are amenable to experimental scrutiny by the introduction of selective perturbations.

Initial studies of cytochrome b_5 focused on the readily available solubilized fragment of the bovine microsomal protein (Strittmatter et al., 1974; Tamburini & Schenkman, 1986) and its apparently identical analogue obtained from erythrocytes (Hultquist et al., 1984). More recently, this protein and several point mutants have been successfully expressed in high yield in *Escherichia coli* by use of a gene synthesized on the basis of the published sequence for the soluble portion of rat cytochrome b_5 (von Bodman et al., 1986; Rogers et al., 1988).

† This research supported by grants from the National Science Foundation, DMB-88-03611, and the National Institutes of Health, HL-22252 and GM-33775.

‡ Current address: Department of Chemistry, Brandeis University, Waltham, MA 02154.

[1] Abbreviations: CoA, coenzyme A; DSS, 2,2-dimethyl-2-pentane-5-sulfonate; NMR, nuclear magnetic resonance; NOE nuclear Overhauser effect; WT, wild type.

0006-2960/91/0430-1878$02.50/0

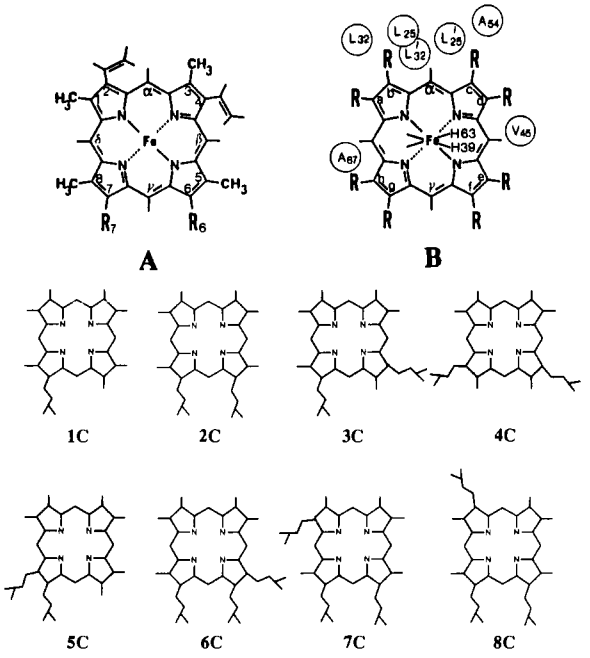

FIGURE 1: (A) Structure of the protohemin skeleton with the potential for modification of the usual propionate sites, i.e., R_6 and R_7; available derivatives are designated **1A–6A** and possess the various R_6 and R_7 groups listed in Table I. (B) The porphyrin skeleton in the protein matrix as elucidated in the crystal structure of bovine cytochrome b_5; all substituents are deleted. Instead, we identify the eight nonequivalent pyrrole positions by the letters a–h referenced to the protein matrix (as reflected by select neighboring amino acid contacts) rather than the heme. For native protohemin, positions a–h are occupied by the substituents 1–8, respectively, in the major form detected in the crystal. We use this labeling scheme to identify where methyls and propionates are located in the protein matrix, and this, in turn, establishes the orientation of a particular hemin. (C) Isomers of the general complex (propionate)$_n$(methyl)$_{8-n}$porphine–iron(III) with n = 1–3, whose structures are depicted in **1C–8C**. The particular orientation of each of the hemins was selected to correspond to the equilibrium orientation, where stable reconstitution complexes result, established by ^{1}H NMR, viewing the hemes from the same perspective as in panel B.

Variations of the surface charges by site-directed mutagenesis have provided a wealth of information on the nature of the interprotein interaction (Rogers et al., 1988). The control of redox potential and the nature of the protein–heme binding, however, can also be pursued effectively by "mutation" of the heme instead of the protein (Brunori et al., 1971; Reid et al., 1984, 1986; Mauk & Mauk, 1986), and in certain cases, this allows the introduction of more varied perturbations. Such perturbations of the heme peripheral carboxylate substituents are readily affected by total synthesis (Smith et al., 1981; Smith & Craig, 1983; Pandey et al., 1987) and allow not only the selective removal of the individual carboxylate side chains of the native protohemin but also the alteration of their lengths and the introduction of additional carboxylate side chains at nonnative positions.

We seek here to characterize structurally in solution the holoproteins of wild-type (WT) rat apocytochrome b_5 reconstituted with a variety of carboxylate-perturbed hemins designed to modify redox potential. The perturbed hemins based on the native protohemin skeleton [A in Figure 1; native protohemin (**1A**) has R_6 = R_7 = propionate] have the two propionates replaced, one at a time, by methyls, **2A** (R_6 = methyl, R_7 = propionate) and **3A** (R_6 = propionate, R_7 = methyl), and the carboxylate chains either shortened, **4A** (R_6 = R_7 = acetate), or lengthened, **5A** (R_6 = R_7 = butyrate). The one previous reported perturbation involves simple esterification of the native propionates, **6A** (R_6 = R_7 = methyl propionates) (Reid et al., 1984; Hartshorn et al., 1987; Funk et al., 1990). Native protohemin (**1A**), however, exhibits extensive heme orientational disorder in the pocket of cytochrome b_5 (Keller & Wüthrich, 1980; La Mar et al., 1981; McLachlan et al., 1986) with the alternate orientations identical in propionate–protein contacts but differing in vinyl–protein contacts, with the two isomers exhibiting measurably different redox potentials (Walker et al., 1988). In the case of rat cytochrome b_5, the problem is particularly severe, with the equilibrium ratio of isomers only ~1.6 (Lee et al., 1990). To eliminate the orientation control of vinyl–protein contacts, we extend the hemin peripheral perturbations to a series of synthetic hemins based on skeleton C in Figure 1, whose asymmetry, if any, is determined solely by the disposition of the propionate groups of interest, i.e., isomers of (propionate)$_n$(methyl)$_{8-n}$porphine–iron(III) (n = 1–3). These include the symmetric analogue to protohemin, **2C**, the hemin with a single propionate, **1C**, isomeric hemins possessing two propionates on either the same, **5C** or adjacent pyrroles, **3C** and **4C**, and the three isomers possessing the native pair of propionates adjacent to the same meso position as well as a third propionate at each of the three isomeric positions, **6C**, **7C**, and **8C**. Only for the symmetric hemic **2C** is the structure of the protein complex expected to be unique with propionate contacts unperturbed from those of the native protein.

We report here on the ^{1}H NMR resonance assignments of the cytochrome b_5 complexes reconstituted with hemins **1A–5A** and **1C–6C** (**7C** and **8C** failed to reconstitute) which, in turn, determine the orientation of the hemin and its peripheral propionate side chain(s) using the nuclear Overhauser effect, NOE (Neuhaus & Williamson, 1989), as discussed in detail previously (La Mar et al., 1986; McLachlan et al., 1988). The questions we address in this paper are as follows: (1) Are the structures homogeneous at equilibrium? (2) What is the heme orientation at equilibrium? (3) What is the structure of transient species formed during the reconstitution? (4) What are the intrinsic preferences for propionate orientation(s) in the heme pocket? (5) How adaptable is the heme pocket toward nonnative carboxylate side-chain positions? (6) What are the electronic/molecular structural consequences of nonnative propionate location? (7) What are the states of protonation for nonnative propionates?

Experimental Procedures

Sample Preparation. Wild-type, WT, rat cytochrome b_5 was prepared by expression of a plasmid-contained synthetic gene coding for the soluble domain of rat cytochrome b_5 in a bacterial host (von Bodman et al., 1986). It was purified as described previously (von Bodman et al., 1986) but did not require an initial trypsin digest, as it is expressed without the hydrophobic "tail" portion. The purified rat protein used in this study had a optical purity index (A_{412}/A_{280}) of ~5.6. Apoprotein was prepared according to reported procedures (Teale, 1959; Reid et al., 1984). Apocytochrome b_5 solution was prepared by dissolving lyophilized apocytochrome b_5 in chilled aqueous 0.2 M phosphate buffer solution (pH ~7); the precipitate, if any, was removed by centrifugation. The modified hemins (**2A–5A**, **1C–6C**) used in this study were synthesized chemically as described previously (Smith & Craig, 1983; Smith et al., 1981; Pandey et al., 1987); protoporphyrin IX was prepared by removal of the iron from hemin **1A** (Fuhrhop & Smith, 1975). The solutions of hemins **5A**, **3C**, **6C**, and **8C** were made by dissolution in 0.2 M NaO^{2}H of ^2H_2O. Other modified hemins used in this study were insufficiently soluble in alkaline aqueous medium. Therefore, a 50% aqueous pyridine/KCN solution was used to dissolve

hemins **2A–4A**, **1C**, **2C**, **4C**, and **5C** (La Mar et al., 1986). Each protein was reconstituted in situ by addition to the chilled apoprotein solution of 1 molar equiv of the chilled hemin solution dropwise with continuous stirring. The holoprotein reconstituted with chemically modified hemin was immediately frozen and lyophilized to remove the pyridine, resulting in trapping of the initially formed species. The lyophilized proteins reconstituted with chemically modified hemins were dissolved in 0.1 M deuterated phosphate buffer solution and centrifuged to remove any insoluble material. The samples were concentrated to ~0.5 mM solution. All the above operations were carried out at 4 °C. The pH was measured with a Beckman 3550 pH meter equipped with an Ingold 620 microcombination electrode; pH values were uncorrected for the isotope effect. The pH of all samples was altered by adding ^{2}HCl or NaO^{2}H as necessary. ^{1}H NMR spectra of the reconstituted holoprotein were taken immediately (<30 min) after dissolution in deuterated phosphate buffer solution.

Optical Spectra. Optical spectra were observed for apoprotein titrated with modified hemin at ambient temperature on a Hewlett-Packard 8540A UV–visible spectrophotometer using 1-cm light path quartz cells referenced against water. The 1:1 heme:apoprotein stoichiometry of protein titrated with modified hemin was determined by monitoring characteristic Soret bands upon conversion of hemin (Ozols & Strittmatter, 1964) ($\lambda \sim 404$ nm) to holoprotein ($\lambda \sim 414$ nm). Optical titration spectra of apoprotein with hemins **4C**, **7C**, and **8C** and protoporphyrin IX (hemin **1A** without iron) failed to exhibit any changes upon mixing, either for this hemin or apoprotein at pH 6–10.

^{1}H NMR Spectra. ^{1}H NMR spectra were recorded at 5–35 °C on a Nicolet NT 500-MHz spectrometer operating in the quadrature mode at 500 MHz. Data were collected by use of double precision on 16 384 data points over a ±15-kHz sweep width with ~3000 transients. The time-evolution spectra of each sample were recorded until the ^{1}H NMR spectra were time independent over 1 month, and hence, the reconstituted species were assumed to be at equilibrium with respect to the heme orientation. The ^{1}H NMR spectrum of protein reconstituted with hemin **5C** was also collected on a Nicolet NT-360 FT-NMR spectrometer operating at 360 MHz in order to investigate the frequency-dependent line width of the resolved signals (Sandstrom, 1982). Peak line widths were measured by fitting the experimental data to a Lorentzian line shape by utilizing the Nicolet line-shape fitting program NMCCAP.

A nuclear Overhauser effect, NOE, difference spectrum was recorded by application of a presaturation pulse of 200 ms with decoupler on-resonance and subtracting it from a corresponding reference spectrum collected under identical conditions but with the decoupler pulse off-resonance; on- and off-resonance frequencies were alternated every 128 scans (La Mar et al., 1986; McLachlan et al., 1988). Typical spectra consisted of at least ~3000 transients with a repetition rate of 1.4 s^{-1}. Chemical shifts were referenced to the residual water resonance, which in turn was calibrated against internal 2,2-dimethyl-2-silapentane-5-sulfonate (DSS). The signal-to-noise ratio was improved by apodization of the free induction decay, which introduced a 10–20-Hz line broadening.

Results

Binding of Hemins. The reaction of equivalent amounts of apocytochrome b_5 and hemins **2A–6A**, **1C–3C**, **5C**, and **6C** in each case gave clear evidence of forming holoproteins with 1:1 heme:apoprotein stoichiometry and with spectral properties (see supplementary material; see paragraph at end of paper regarding supplementary material) very similar to those of the native protein (Ozols & Strittmatter, 1964). Thus for these hemins, the characteristic Soret shifts from 404 to 414 nm upon reconstitution, as observed for native protohemin, **1A** (not shown) (Ozols & Strittmatter, 1964). The optical titrations displayed well-defined breaks at 1:1 stoichiometry indicative of relatively strong heme binding. The incorporation of these hemins into the heme pocket is also verified by the observations of ^{1}H NMR spectra clearly indicative of heme–protein contacts largely unperturbed from those of the native protein (see below). On the other hand, titration of apocytochrome b_5 with hemin **4C**, **7C**, or **8C** (at weakly acidic to alkaline pH) failed to exhibit changes in either the hemin or apocytochrome b_5 absorbance and yielded ^{1}H NMR spectra reflective of the apoprotein (not shown). A similar lack of optical and NMR spectral perturbations was observed upon reaction of apocytochrome b_5 with protoporphyrin IX (i.e., **1A** with the iron removed). Hence, we conclude that the iron–His bonds are essential to heme binding and that certain unnatural arrangements of heme propionates strongly inhibit the binding of the heme in the pocket.

Orientation of Protohemin IX Derivatives. The resolved portions of the ^{1}H NMR spectra of native rat cytochrome b_5 and the complexes of its apoprotein with hemins **1A**, **2A**, **3A**, **4A**, and **5A** are illustrated in spectra A, B, C, D, and E of Figure 2, respectively. The assigned resonances for the heme orientation with vinyl contacts as in the X-ray-detected heme orientation (Mathews et al., 1979) of largely isostructural bovine cytochrome b_5 are labeled M_i, H_i, and V_i and those of the orientation with the heme rotated by 180° about the α,-γ-meso axis are labeled m_i, h_i, and v_i, on the basis of the designation for methyls (M_i, m_i), vinyls (V_i, v_i), and carboxylate α-protons (H_i, h_i). The hyperfine (largely contact) shifts for heme substituents are known to depend predominantly on, and very sensitively to, not so much their position on a given heme but to the position in the protein matrix (Mathews et al., 1979). This is due to the fact that the contact shift pattern for low-spin iron(III) reflects the unpaired spin distribution of the ferric spin whose orbital ground state is predominantly controlled by the protein-based rhombic perturbation involving the imidazole orientation(s) of the axial His (Shulman et al., 1971; La Mar, 1979; La Mar et al., 1986). Within a native polypeptide folding pattern, the axial His orientations remain essentially constant and hence lead to contact shifts diagnostic of the particular position on the heme skeleton relative to this protein matrix. The invariant heme substituent contact shift pattern for perturbed hemes has been documented for both myoglobin (La Mar et al., 1986) and cytochrome b_5 (La Mar et al., 1981; McLachlan et al., 1988). Conversely, if a significantly altered heme contact shift pattern is established for a modified hemin, then the heme–protein contacts controlling the electronic/magnetic properties are altered. The empirical strategy that allows determination of orientation from assignments (or vice versa), as determined from extensive studies of systematically perturbed hemes in cytochrome b_5 (La Mar et al., 1981; Keller & Wüthrich, 1981; McLachlan et al, 1988), is reproduced in panel F of Figure 2.

The removal of the 6-propionate (hemin **2A**) leads to a single orientation with a vinyl at position b (peaks V_b^{α}, V_b^{β}), which is missing peaks H_f, H_f' (Figure 2B), dictating that there is a vinyl at position b and no propionate at position f; hence, the only detectable orientation ($K > 30$) has the vinyl contacts as found in the X-ray structure (Mathews, 1980), with the 7-propionate link to the protein unaltered. On the other hand, selective removal of the 7-propionate (hemin **3A**) does not lead

Table I: Chemical Shifts of WT Rat Ferricytochrome b_5 Complexes Reconstituted with Prototheme Derivatives[a]

resonance[c]	1A,[b] R_6 = P, R_7 = P	2A, R_6 = M, R_7 = P	3A, R_6 = P, R_7 = M	4A, R_6 = A, R_7 = A	5A, R_6 = B, R_7 = B
1	10.73 (−0.64)[d]	10.80		10.05	
2	27.43 (10.82)	27.42	11.12	25.24	25.51 (13.09)
3	14.44 (31.81)	14.90	31.61	15.00 (29.43)	14.75 (29.53)
4	5.10 (16.84)		17.00		
5	20.42 (1.30)	20.82		19.26	18.80
6	14.98 (18.84)	32.86	18.24	14.49	13.24 (15.98)
7	19.59 (15.32)	18.91	33.65	18.65	22.37 (15.06)
8	2.90 (24.29)		24.98	(25.24)	(21.62)
H_{39}	16.33 (16.33)	16.32	16.26	16.12	16.32
L_{46}	−2.49 (−3.08)	−2.28	−3.10	−2.23	−2.48
P_{40}	−3.40 (−3.27)	−3.62	−4.34	−3.19	−3.32
K_{eq}[e]	~1.6	>30	<0.03	~1.7	~3.8

[a] Shift in ppm from DSS in ^2H_2O solution at 25 °C and pHs described in the caption to Figure 1. [b] Structure of hemin shown in Figure 1; M, P, A, and B refer to methyl, propionate, acetate, and butyrate side chains, respectively. [c] Numbered positions are for the heme substituents as shown in panel A of Figure 1; the amino acid signals are for the His 39 $C_\beta H$ (H_{39}), Leu 46 $C_{\delta_2}H_3$ (L_{46}), and Pro 40 $C_\beta H$ (P_{40}). [d] Shifts for the equilibrium minor isomer (when observed) are given in parentheses. [e] K_{eq} for forming isomer with vinyls oriented as in the X-ray crystal structure.

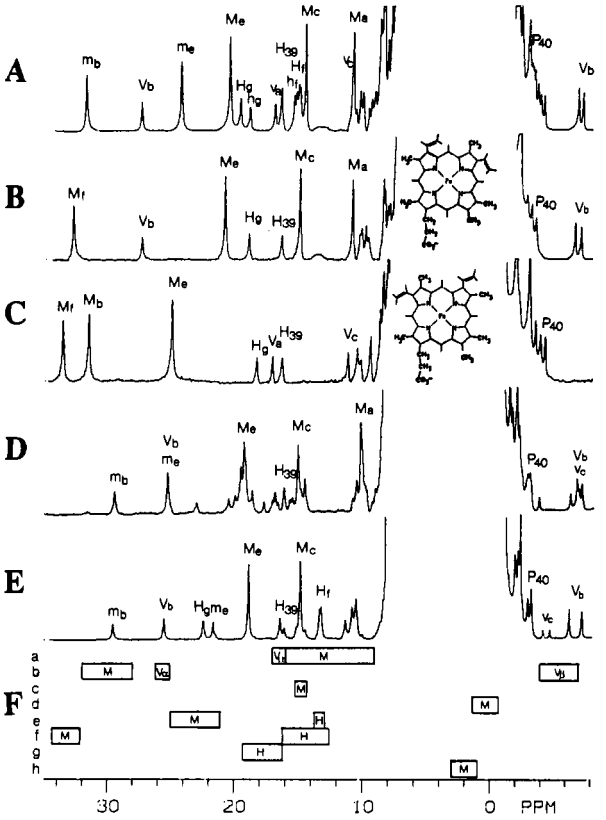

FIGURE 2: Resolved portions of the ^1H NMR spectrum of equilibrated WT rat cytochrome b_5 in ^2H_2O at 25 °C, reconstituted with the following: (A) native protohemin (**1A**) at pH 7.41; (B) 6-methyl-6-despropionate hemin (**2A**) at pH 7.55; (C) 7-methyl-7-despropionate hemin (**3A**) at pH 7.73; (D) hemin **4A** with the native propionates replaced by acetates at pH 7.66; (E) hemin **5A** with the native propionates replaced by butyrates at pH 7.32. Peak designations are M_i,m_i (methyls), V_i,v_i (vinyl protons), and H_i,h_i (propionate H_αs) with the subscript i = a–h to designate the position of the group in the protein matrix in the labeling scheme of panel B in Figure 1; M_i,V_i,H_i and m_i,v_i,h_i arise from the heme disorder isomers with vinyl contacts as in the crystal structure and those rotated by 180° about the α,γ-meso axis. (F) Empirical correlation of chemical shifts for methyls (M_i), vinyls (V_i), and propionate H_αs with positions in the protein matrix by use of the labeling scheme i = a–h as described in panel B of Figure 1.

to a vinyl at position b, and moreover, there is a methyl at position f (Figure 2C). This requires that the only detectable species in solution ($K > 30$) has the vinyl contacts reversed from those of the X-ray structure, this time with the 6-propionate oriented to form the internal link to the protein. In the case of shortening both carboxylates to acetates (hemin **4A**) or lengthening both to butyrates (hemin **5A**), we observe the same set of two peaks (spectra D and E of Figure 2, respectively) as for native protein, but with slightly perturbed shifts and ratio of the same two heme rotational isomers. The chemical shift values of the peaks assigned for individual heme orientation with the empirical correlation illustrated in Figure 2F, and as quantitatively confirmed by diagnostic steady-state NOEs (not shown) (McLachlan et al., 1988), are listed in Table I.

Orientations of (Propionate)$_n$(methyl)$_{8-n}$porphine–Iron(III) Derivatives. The strategy for the assignment of the resonances and determination of the orientation is made with the heme methyl and propionate H_α shift correlation of Figure 2F, as supported by the steady-state NOEs needed to resolve potential ambiguities. The assignment of resonances is made not with respect to the hemin but with respect to the position in the protein matrix, according to the labeling scheme described in Figure 1B. The NOE strategy involves sequential methyl assignments based on ca. −5% NOEs between adjacent methyls on the same pyrrole and ca. −1% NOEs between pairs of methyls adjacent to the same meso position, as discussed in detail for a variety of myoglobin complexes, including that with hemin **2C** (La Mar et al., 1986). Key dipolar contacts to hyperfine-shifted amino acid signals from the protein matrix are based on our previous demonstration of such diagnostic NOEs for a number of sites in the proton matrix, as observed for the native bovine cytochrome b_5 by both steady-state NOEs and 2D NOESY peaks (McLachlan et al., 1988). Both the characteristic heme intermethyl NOEs and diagnostic heme–protein NOEs are given in the supplementary material for the symmetric heme **2c**, which must have the two propionates oriented as in the crystal structure.

The resolved portions of the ^1H NMR spectra of the protein complexes formed initially after reconstitution with monopropionate heptamethylporphine–iron(III), hemin **1C**, and after extensive equilibration are illustrated in panels A and C of Figure 3, respectively. Two sets of methyl (M_i, m_i) and single-proton (H_i, h_i) peaks are observed initially, with the set of M_i,H_i gaining intensity at the expense of set m_i,h_i, reaching an equilibrium ratio M_i/m_i of ~25. Computer subtraction of the equilibrium trace (Figure 3C) from the initial spectrum (Figure 3A) yields the trace for the intermediate in the reconstitution, as shown in Figure 3B. The empirical correlation in Figure 2F identifies methyls at positions a, b, c, e, and f, indicating that *the sole propionate is at position g* (turned into the protein) rather than f (extended into solution). This orientation is quantitatively established by the NOE data in Figure 3D–G, which demonstrate the characteristic NOE pattern between the geminal propionate C_αHs at position g (Figure 3D). The expected −5% NOEs between M_f and M_e,

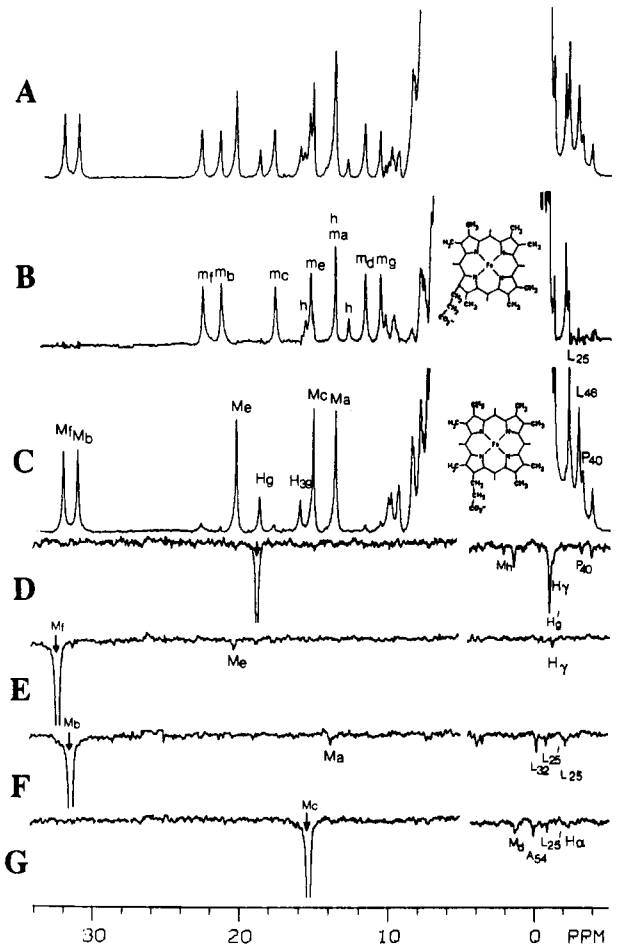

FIGURE 3: Resolved portions of the 500-MHz ^1H NMR spectra of WT ferricytochrome b_5 in ^2H_2O, pH 7.48, at 25 °C, reconstituted with the monopropionate hemin **1C**: (A) immediately after reconstitution, showing two species, and (B) computer difference trace for the intermediate by subtracting trace C from trace A, showing peaks m_i,h_i; (C) at equilibrium with peaks M_i,H_i. (D–G) NOE difference traces obtained by subtracting the reference trace C from a trace with one peak saturated (indicated by vertical arrow). (D) Saturate H_g; note large NOE to H_g' indicative of geminal CH_2, as well as NOEs diagnostic of g positions; in particular to peak γ shown to arise from γ-meso-H in native protein. Peaks M_h and P_{40} arise from 8-CH_3 and Pro 40 $C_\beta H$, respectively. (E) Saturate M_f; note ca. −5% NOE to M_e and small NOE to meso-H peak H_γ. (F) Saturate M_b; note ca. −5% NOE to M_a and NOEs to L_{32} (Leu 32 $C_{\delta_2}H_3$), L_{25}' (Leu 25 $C_{\delta_2}H_3$), and L_{25} (Leu 25 $C_{\delta_1}H_3$) diagnostic of position b. (G) Saturate M_c; note ca. −5% NOE to M_d as well as NOEs to A_{54} (Ala 54 $C_\beta H_3$), L_{25}' (Leu 25 $C_{\delta_2}H_3$), and H_α (α-meso-H) (McLachlan et al., 1988).

M_b and M_a, and M_c and M_d are shown in panels E, F, and G of Figure 3, respectively, and the common NOE of H_g (Figure 3D) and M_f (Figure 3E) to meso-H peak Hγ identifies neighboring pyrrole methyl resonances (McLachlan et al., 1988). It is noted here that the contact shift pattern for the intermediate (Figure 3B) is modified from that predicted by the empirical correlations from a largely unperturbed electronic/molecular structure (Figure 2F). Unfortunately, the lifetime for this species is too short even at 4 °C to assign resonances, and the hemin is available in too small a quantity to critically evaluate all conditions that could stabilize the intermediate. Hence, the orientation of the intermediate could not be determined experimentally.

The ^1H NMR traces for the initial complexes and the equilibrium complex formed between apocytochrome b_5 and hemin **3C** are given in panels A and B of Figure 4, respectively, with the computer-difference trace for the intermediate given in Figure 4C. The empirical methyl shifts in Figure 2F identify

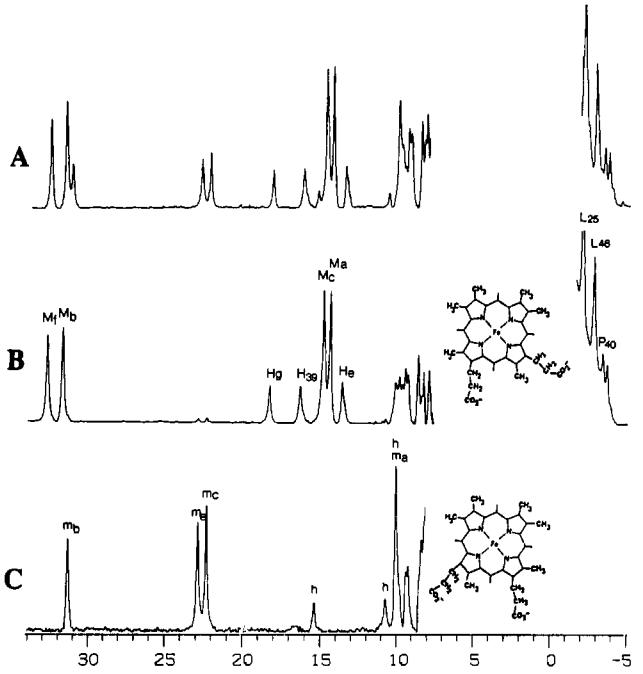

FIGURE 4: Resolved portions of the 500-MHz ^1H NMR spectra of WT rat cytochrome b_5 reconstitute with heme **3C**, in ^2H_2O, 25 °C, pH 7.77: (A) immediately after reconstitution showing two species, M_i and m_i, and (D) after equilibrium has been reached and primarily peaks M_i,H_i remain. (E) Computer-generated difference trace for transient isomer, with peaks m_i,h_i obtained by subtracting trace B from trace A. Subscripts a–h designate position of substituent in B of Figure 1. The assignment of set M_i is by NOEs; the set m_i for the intermediates is assigned with the empirical correlation in Figure 2F.

methyls at positions a, b, c, and f for the equilibrium complex, which indicates propionates at positions e and g at equilibrium. Detailed NOE studies quantitatively support this, in particular the diagnostic NOE between propionate geminal proton H_g and H_g' (not shown), as found above in Figure 3D for hemin **1C**. The intermediate in Figure 4C again has too short a lifetime to obtain useful NOEs, but the empirical shift correlation indicates methyl at positions a, b, c, and e but no methyl at position f; this dictates the heme orientation with propionates at positions f and h. The ^1H NMR traces shortly after reconstitution and at equilibrium of apocytochrome b_5 reconstituted with the sole tripropionate hemin found to incorporate into the heme pocket, hemin **6C**, are shown in panels A and B of Figure 5, respectively. The computer difference generated trace for the reconstitution intermediate is given in Figure 5C. The empirical methyl shift correlation, as supported by NOEs (not shown), clearly establishes the absence of a methyl at position e at equilibrium and places the three propionates at positions e, f, and g. The intermediate in Figure 5C again is also too short lived for NOEs, but the empirical shift correlations argue for methyls at positions a, b, c and e, indicating that propionates occupy positions f, g, and h. The chemical shifts are listed in Table II.

The resolved portions of the neutral pH ^1H NMR spectrum of the single detectable complex observed upon reconstitution of apocytochrome b_5 with the hemin with both propionates on the same pyrrole, hemin **5C**, is illustrated in Figure 6A. It exhibits all six methyl peaks as resolved signals but with a contracted spread in chemical shift. Hence, the molecular/electronic structure is perturbed, and the empirical correlation of Figure 2F appears to be of little utility in deducing assignments and orientation. However, with only two single protons downfield of 10 ppm, the pattern suggests the absence of a propionate at position f and, hence, an orientation with

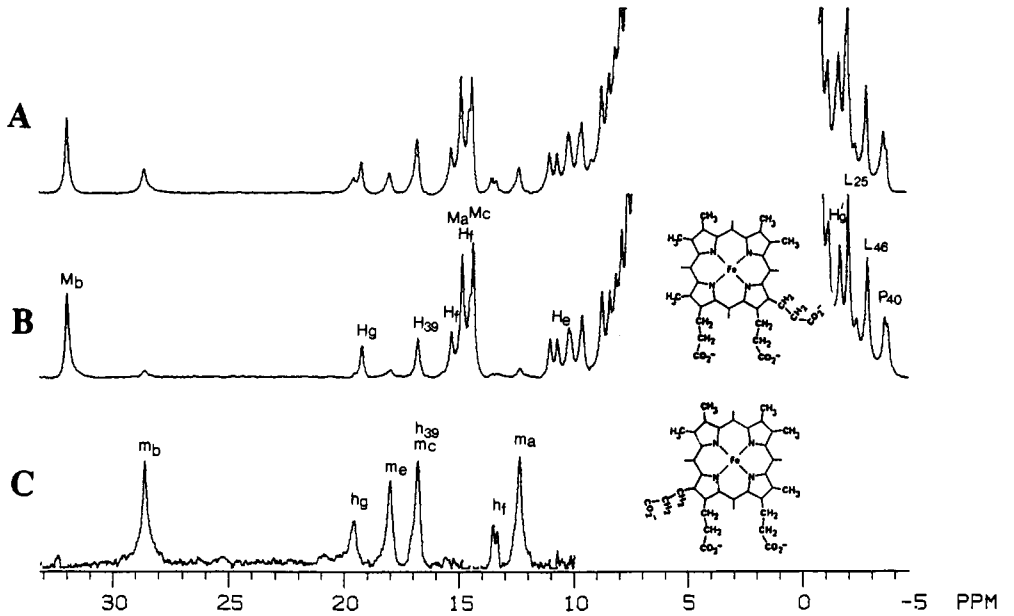

FIGURE 5: Resolved portions of the 500-MHz ^1H NMR spectra of WT rat ferricytochrome b_5 reconstituted with the tripropionate hemin **6C**, in ^2H_2O, pH 7.19 at 25 °C: (A) immediately after reconstitution, showing two species with two sets of peaks; (B) after equilibrium has been reached and primarily the species with peaks M_iH_i remains. (C) Difference spectrum for the intermediate, with peaks m_ih_i obtained by subtracting trace B from trace A. Subscripts a–h designate substituent position in panel B of Figure 1. The equilibrium complex peaks M_iH_i are assigned by NOEs; these form the intermediates m_ih_i assigned on the basis of the empirical correlation in Figure 2F.

Table II: Chemical Shifts for WT Rat Ferricytochrome b_5 Complexes Reconstituted with (Propionate)$_n$(methyl)$_{8-n}$porphine–Iron(III) Derivatives[a]

hemin position[b]	1C[c]	2C	3C	5C	6C
a	13.68 (13.68)[d]	13.42	14.44 (10.13)	13.09	14.28 (12.27)
b	31.25 (21.78)	31.73	31.83 (31.41)	20.87	31.88 (28.52)
c	15.16 (17.80)	14.87	14.88 (22.39)	18.07	14.75 (16.68)
d	1.29 (11.70)	1.30	1.21	12.06	1.02
e	20.36 (15.41)	19.87	13.65 (22.95)	15.48	10.62 (17.91)
f	32.24 (22.77)	15.05	32.83 (10.85)	21.55	15.20 (13.45)
g	18.76 (10.65)	19.59	18.35	16.43	19.12 (19.46)
h	2.10	1.97	2.19		1.68
H_{39}[e]	16.04	16.21	16.36	14.25	16.68
L_{46}[e]	−2.91	−3.02	−2.92	−1.26	−2.89
P_{40}[e]	−3.85	−3.27	−3.78	−1.63	−3.89

[a] Shifts in ppm from DSS in ^2H_2O solution at the temperatures and pHs described in the captions to Figures 3–6. [b] Hemin positions referred to their location in the protein-based labeling scheme in panel B of Figure 1. [c] Hemin structure as shown in panel C of Figure 1. [d] Shifts for reconstitution intermediate, if observable, are shown in parentheses. [e] Select resolved amino acid signals labeled as in Table I and Figures 2–6.

propionates at positions g and h. Detailed NOE data presented in Figure 6 quantitatively confirm both this orientation and the fact that the pattern of methyl shift is still consistent with that predicted by the empirical correlation (Figure 2F), although the spread is considerably reduced. The ca. −5% NOEs from M_b to M_a (Figure 6B) and from M_c to M_d (Figure 6C) identify pairs of adjacent methyls and the common NOE to α-meso-H (peak H_α) places them on adjacent pyrroles. The ca. −5% NOE from M_f to M_e locates the other pair of adjacent methyls (Figure 6D) and also yields an NOE to meso-H (peak H_γ) (McLachlan et al., 1988). Common NOEs to β-meso-H at 7 ppm are observed from both M_e and M_d (not shown). The large NOE indicative of a geminal methylene of a propionate, as well as an amino acid NOE pattern diagnostic position g, is observed upon saturation of H_g (Figure 6E), and its NOE to signal H_γ determins the remainder of the unique assignments (McLachlan et al., 1988). Hence, the two propionates occupy positions g and h in the protein matrix in the only detectable complex formed during the resolution of hemin **5C**.

The temperature dependence of the hyperfine-shifted signals of the equilibrium products of the reconstitution of apo-

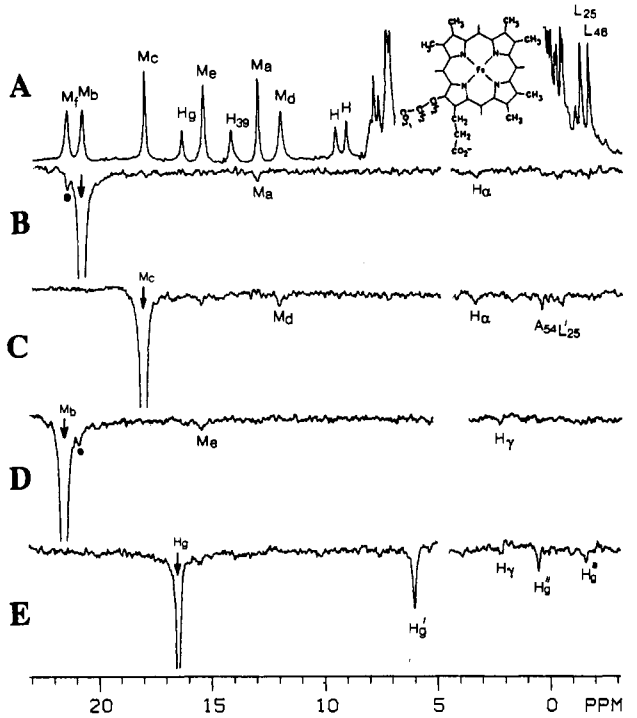

FIGURE 6: (A) Resolved portions of the 500-MHz ^1H NMR spectra of WT rat ferricytochrome b_5 reconstituted with hemin **5C**, in ^2H_2O, pH 7.77 at 35 °C; the trace is invariant with time and reflects a single species. Subscripts a–h designate substituent position in panel B of Figure 1. (B–F) NOE difference trace obtained by subtracting the reference trace in (A) from traces with a peak saturated (indicated by vertical arrow): (B) saturate M_b; note ca. −5% NOE to M_a and NOE to meso-H peak H_α; (C) saturate M_c; note ca. −5% NOE to M_d and NOE to meso-H peak H_α, A_{54} (Ala 54 $C_\beta H_3$), and L_{25}' (Leu 25 $C_{\delta_2}H_3$); (D) saturate M_f; note ca. −5% NOE to M_e and NOE to meso-H peak H_γ; (E) saturate H_g; note ca. −30% NOE to H_g' (geminal partner to H_g) and NOEs $Hg''(7\text{-}H_\beta)$, $Hg'''(7\text{-}H_{\beta'})$, and meso-H peak H_γ diagnostic of position g (McLachlan et al., 1988).

cytochrome b_5 with all hemins except **5C** exhibited slopes for which the data for hemin **1C** are representative (Figure 7A) and are essentially the same as those for the native protein (Burns, 1978) or that reconstituted with hemin **2C** which

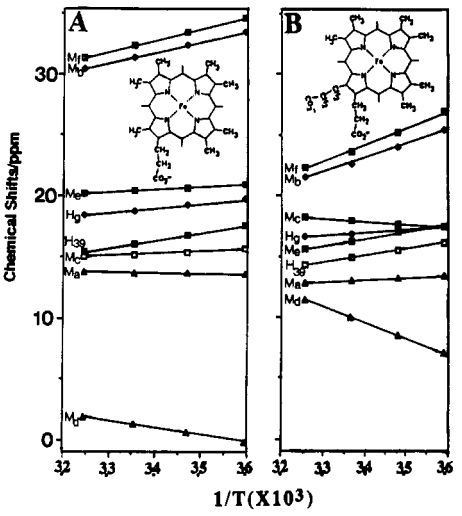

FIGURE 7: Plots of chemical shift versus reciprocal temperature (Curie plot) for heme substituent peaks (M_i,H_i) labeled as described for Figures 3 and 6 and axial His 39 peak H_{39} for WT and ferricytochrome b_5 reconstituted with (A) hemin **1C** and (B) hemin **5C**. Note the anomalous slopes for peaks M_f, M_b, M_c, and M_d in (B).

retains the native propionate contacts (not shown). In contrast, the temperature dependence of the shift (Curie plot) for the complex with hemin **5C** exhibits several anomalies, such as significantly enhanced slopes for some signals (i.e., M_f, M_b, and M_d) or reversed slopes for the same sign shift (M_c), as shown in Figure 7B. Moreover, the line widths for the various methyl peaks for the protein complex of hemin **5C** differ, with the M_d, M_b and M_f methyl peaks some 50% broader than the M_c, M_e and M_a peaks at 500 MHz. At the lower field of 360 MHz, the lines M_d, M_b, and M_f selectively become narrower (not shown), indicating some dynamic process in the fast-exchange limit.

The pH dependence of the hyperfine-shifted peaks between 5 and 10 were determined for the equilibrated complexes of the monopropionate, heptamethyl isomer, hemin **1C** (Figure 8A), the hemin with propionates in the same pyrrole, hemin **5C** (Figure 8B), and hemin **3C** (Figure 8C), as well as **2C** (not shown). Only the complex of hemin **5C** exhibited pronounced pH effects on all heme substituent shifts, in contrast to both the other hemins and the native protein (McLachlan et al., 1986a,b).

Discussion

Heme–Protein Binding. The binding free energy of hemins to *b*-type hemoproteins generally consists of contributions from the axial ligand–iron bond(s), salt bridges, or hydrogen bonds between the ubiquitous propionates and the protein matrix and attractive dispersion interactions between the polarizable heme system and hydrophobic amino acid side chains. For myoglobin, both the salt bridges (Tamura et al., 1973) and the His–iron bond (Jameson et al., 1984) can be abolished while strong prosthetic group binding in a largely unperturbed pocket is still retained (Tamura et al., 1973; Jameson et al., 1984; Krishnamoorthi & La Mar, 1984; La Mar et al., 1989). Moreover, it is possible to reconstitute myoglobin with hemins that place propionates at each of the eight possible sites in the protein matrix and still retain tight heme binding in a largely unperturbed native heme pocket structure (Hauksson et al., 1990).

Cytochrome b_5 fails to bind heme upon abolishment of the axial bonds for metal-free protoporphyrin IX, as reported previously (Ozols & Strittmatter, 1964), indicating a considerably smaller contribution to prosthetic group binding from the peripheral protein contacts than for myoglobin. Moreover,

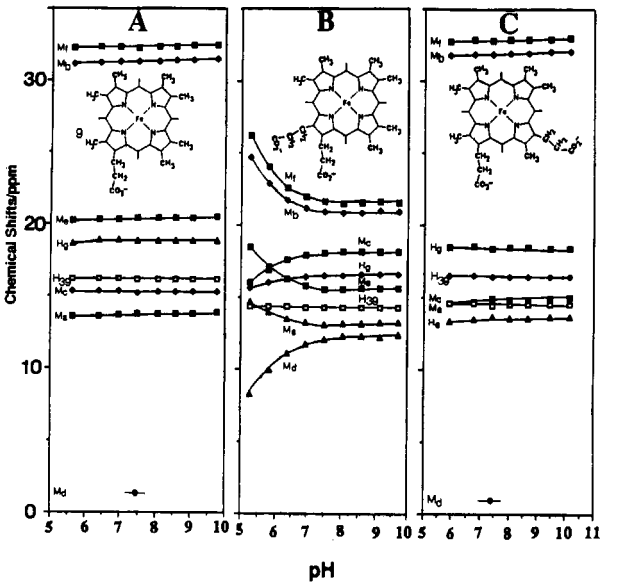

FIGURE 8: Plots of heme substituent (M_i,H_i) and select amino acid peak H_{39} (His 39 $C_\beta H$) versus pH, in ^2H_2O, at 25 °C, for WT rat ferricytochrome b_5 reconstituted with: (A) hemin **1C** with the sole propionate at position g, (B) hemin **5C** with the two propionates at positions g and h, and (C) hemins **3C** with the two propionates at positions e and g. Peak labeling is the same as given in Figures 3, 4, and 6.

the heme pocket can accommodate propionates at sites e, f, g, and h, albeit reluctantly and not simultaneously at e and h, *but not at all the interior positions a, b, c, and d*, as evidenced by the complete absence of binding of hemins **7C** and **8C**. While the steric constraints imposed on the larger propionate groups may be part of the reason, at least a major contribution to the reduced binding constant must be due to the inability to accommodate in the pocket interior the polar nature of the propionates. Thus, the derivative 2,4-diisobutenyldeuterohemin, which has the same structure as protohemin **1A** except that the vinyls are placed by $(CH_3)_2C{=}CH{-}$ groups, readily reconstitutes into apocytochrome b_5 with the isobutenyl group placed solely at the b and d positions where the vinyls are found in the X-ray structure (Lee et al., 1990). Hence, at least the b and d positions can accommodate such bulky groups if they are nonpolar. We therefore conclude that the interior of the heme pocket of cytochrome b_5 is less polar and sterically less adaptable than that of myoglobin (Hauksson et al., 1990).

Equilibrium Carboxylate Side-Chain Orientations. The unique orientation of hemin **1C** dictates that the g position allows by far the strongest propionate–protein link and involves a pair of hydrogen bonds to the NH and OH of Ser 64 in the crystal structure (Mathews et al., 1979). Thus, the removal of the 6-propionate in hemin **2A** leaves the vinyl contacts as in the crystal, since both the propionate and vinyl contacts favor this orientation. Since the protohemin derivative with the 7-propionate missing, hemin **3A**, yields a unique orientation with the vinyls reversed from that found in the crystal, the preference of the propionate for position g over f is greater than that of the vinyl at positions b and d over a and c. Similarly, the unique orientation of hemin **6C** shows a strong ($K_{eq} = \sim 15$, $\Delta G = \sim 1.6$ kcal) preference for position e over h. However, since hemin **3C** has propionates occupying only positions e and g, the preference for the g over h position must be much larger than that of the e over g position. The greater preference for the e over h propionate orientation can be rationalized by a computer graphics visualization that suggests the propionate at the e or 5–methyl position of the native hemin

may extend into solution. The importance of the protein link for a propionate at position g is also indicated by the observation that, while propionates at positions g and h (hemin **5C**) or positions g and c (hemin **3C**) allow formation of a stable 1:1 heme–protein complex, the restriction to allow the occupation of propionates only at positions e and h (hemin **4c**) renders the holoprotein complex unstable in solution.

Carboxylate pKs. The pH titration of the ^{1}H NMR spectrum of native cytochrome b_5 reveals significant shift changes only for the 6-propionate α-CH_2 and, to a lesser degree, for the adjacent 5-CH_3 peaks (Keller & Wüthrich, 1980). This has been interpreted in terms of a pK of ~5.9 for the 6-propionate (f position) group (McLachlan et al., 1986a). The absence of any pH influence on shifts for the protein complex with monopropionate heptamethylporphyrin–iron(III), **1C** (Figure 8A), with only the propionate link to Ser 64, confirms the titration of the 6-propionate in the native protein. Moreover, the hydrogen-bonding network involving the internal (g position) propionate observed in the crystal structure (Mathews et al., 1979) must be maintained over the complete pH range 5–9.5. (Since the pair of acceptor hydrogen bonds with Ser 64 dictate an ionized carboxylate, the pK must be <5 for the g or crystallographic 7-propionate.) The pH profile for the protein complex of hemin **3C** reflects only very weak pH dependence with the largest shift change observed at low pH for H_e, the propionate H_α at the crystallographic 5-methyl position. Inspection of a molecular graphics display of the van der Waals surface of cytochrome b_5 suggests that the "5-propionate" group may have its carboxylate exposed to solvent.

The fact that hemin **5C**, with a propionate at both positions g and h, exhibits dramatic pH effects (Figure 8B), while hemin **1C**, with only the g-position propionate, exhibits no pH effect, indicates that the propionate at position h (at the crystallographic 8-methyl position) titrates below pH 6. However, whether this pK reflects the intrinsic properties of the h-position propionate, that resulting from interaction with the adjacent g-position propionate, or the titration of the g-position propionate is influenced by the adjacent h-position propionate cannot be determined at this time. Moreover, in contrast to the highly localized effects of the single propionate titrations for positions e and f, the pH-modulated change involving the propionate at position h (or simultaneously positions g and h) strongly perturbs all resonances for the heme while leaving those of the protein largely unperturbed (Figure 8B).

Structural Consequences of Nonnative Carboxylate Contacts. The influence of shortening (i.e., acetates in hemin **4A**; Figure 2D) or lengthening (i.e., butyrates in hemin **5A**; Figure 2E) the carboxylate side chains for the native protohemin skeleton on the hyperfine shift pattern is minimal (McLachlan et al,. 1988). Hence, the key structural link to the protein at position g (the crystallographic 7–position) does not appear to depend significantly on the length of the link; even the thermodynamics of heme disorder (K_{eq}) appear largely unperturbed (see Table I).

The hyperfine shift patterns for both the hemin (primarily contact) and amino acid residues (primarily dipolar) for the equilibrated reconstituted proteins are essentially identical for the synthetic hemins **2C**, **3C**, and **6C** and indicate minimal structural perturbations of the heme pocket molecular/electronic structure upon either removal of the solvent-exposed crystallographic 6-propionate at position f (hemin **1C**) or the introduction of an additional propionate into the crystallographic 5-methyl or e position (hemins **3C** and **6C**). In contrast, the introduction of a propionate at the crystallographic 8-methyl or h position (hemin **5C**) significantly contracts the range of heme methyl contact shifts (Figure 6A) as compared to that observed for other hemins, and this perturbation appears to be dependent on both temperature and the state of protonation of the propionate at position h. All of the NMR spectral properties of the cytochrome b_5 complex of hemin **5C** can be interpreted on the basis of an equilibrium between two structures, one with a "normal" hyperfine shift pattern similar to that predicted by the correlation in Figure 2F (designated N) and another with a perturbed electronic/molecular structure characterized by significantly reduced rhombic asymmetry for the heme π-electron distribution (designated P), i.e.

$$(\mathbf{5C}\text{–cytochrome } b_5)_N \rightleftarrows (\mathbf{5C}\text{–cytochrome } b_5)_P \quad (1)$$

The electronic asymmetry difference between hemin **5C** and that of any of the other hemins reconstituted into cytochrome b_5 manifests itself most dramatically for methyls at positions f and b, which are significantly shifted upfield, and the methyl at position d, which is shifted significantly downfield (and is actually resolved from the diamagnetic envelope) compared to that of hemin **2C** or the native protein (Keller & Wüthrich, 1980; La Mar et al., 1981; McLachlan et al., 1988). The ^{1}H NMR trace in Figure 6A shows, moreover, that these methyl signals labeled M_f, M_b, and M_d are significantly broader than the others, and this increased line width is field dependent and hence indicative of a dynamic equilibrium in the fast exchange limit such as described in eq 1 (Sandstrom, 1982). The methyl peaks which must differ most significantly in the two alternative structures (M_f, M_b, M_d) exhibit the largest line broadening. When the temperature is lowered, all lines, but particularly M_f, M_b, and M_d, broaden significantly, as expected (not shown). The anomalous slopes of the shifts in the Curie plot (Figure 7B) also indicate a temperature dependence of the peaks consistent with an equilibrium between the alternative forms in solution. The Curie plot slopes of particularly those methyls exhibiting the anomalous line broadening (M_f, M_c, M_d) are significantly increased so that the low-temperature pattern is much closer to "normal", as observed for hemins **1C** (Figure 7A) and **3C** (not shown). Note in particular the anomalous slopes for M_f, M_d, M_c, and M_d, all of which deviate from "normal" behavior so as to approach the shift values for those methyls in the unperturbed or native electronic/molecular structure. Hence, lowering the temperature shifts the equilibrium in eq 1 to the left.

The equilibrium (eq 1) involving the same two structures appears to be modulated also by the titration of the h-position propionate. Thus the pH profile for the protein complex of hemin **5C** is flat above pH 7, but at acidic pH each resonance approaches the chemical shift for that for any "normal" hemin such as native protohemin or hemins **1C**, **2C**, and **3C** (Figure 8B). The limiting values at low pH cannot be attained because of sample precipitation. However, all incremental shift changes with pH at low pH are approximately proportional to the difference between the high-pH values and those given the the shift correlations in Figure 2F or for "normal" complexes as shown in Figure 8A,C. Hence, protonation of the h-position propionate shifts the equilibrium (eq 1) to the left. Assuming that the limiting shifts for (**5C**–cytochrome $b_5)_N$ would be those typical of the complex with hemin **1C** or **3C** (i.e., the empirical correlation shown in Figure 2F), we estimate that the pH profile for hemin **5C** in Figure 8B reflects a pK of ~5.1 for the propionate at position h.

Hence, we conclude that the anomalous hyperfine shift pattern for the equilibrium cytochrome b_5 complex of hemin **5C** reflects an h-position propionate–protein interaction that

is an alternative to the native g-position propionate–protein link and the alternative link is thermodynamically slightly less stable than the g-position propionate at neutral pH and much less stable when the h-position is protonated. The detailed molecular/electronic structural consequences of the alternate propionate–protein link cannot be defined further with available data except that they result in considerably reduced rhombic electronic asymmetry. Since the asymmetry is dictated by the relative positions of the axial His imidazole plane(s) to the heme N–Fe–N axes (McLachlan et al., 1988), either the perturbed high-pH and/or high-temperature form of the cytochrome b_5 complex with hemin **5C** has the hemin rotated slightly about unperturbed His–Fe–His bonds in order to optimize the h propionate link, or the h-position propionate link perturbs the orientation of one or both of the axial His. Since the Scr 64 is adjacent to one axial His (Mathews et al., 1979), a direct influence on His 63 orientation is reasonable.

Structures of Intermediates and the Reconstitution Mechanism. The hyperfine shift pattern for the reconstitution intermediate for monopropionate hemin **1C** (Figure 3B) exhibits a pattern perturbed from that of the empirical correlation (Figure 2F) or the equilibrium product (Figure 3C) in the same manner as that just defined above for hemin **5C**, except for the presence of the additional methyl peak M_g; i.e., the pattern is likely the same as for "normal" complexes except the range shift is highly contracted. This similarity of the hyperfine shift pattern for the complex of hemin **5C** and the intermediates for hemin **1C** argues that the alternative initial form of the protein complex of hemin **1C** has the lone propionate at position h (i.e., the crystallographic 8-methyl position) rather than the f or crystallographic 6-position. The assignments indicated by peak labeling in Figure 3B are made solely by analogy to those of the hemin **5C** complex in Figure 6A. *Hence, the initial heme disorder is about a porphyrin N–Fe–N rather than a meso–Fe–meso axis*, and the initial heme–protein hydrogen bond can be made for either position g (the stable 7-propionate) or position h. Any other orientation would require a low-field resolved propionate H_α resonance, contrary to observations. Moreover, since the molecular/electronic structural properties are similarly perturbed relative to native cytochrome b_5 for the intermediate hemin **1C** and the equilibrium hemin **5C** complexes, we conclude that the alternative heme–protein link is indeed one involving the h-position propionate rather than a g-position propionate link simply perturbed by the adjacent h-position propionate.

The intermediates in the reconstituted hemin **3C** (Figure 4C) and hemin **6C** were also too short lived to allow NOE assignments. For hemins **3C** and **6C**, however, the observed shifts follow the empirical correlations which predict only four low-field methyls for the orientation with propionates at positions f and h for hemin **3C** and f, g, and h for hemin **6C**. Thus the intermediates for these two hemins exhibit the conventional disorder about the meso–Fe–meso axis (La Mar et al., 1981). It is noted, however, that the intermediates in the reconstitution with hemins **3C** and **6C** exhibit heme methyl contact shift patterns more or less "normal" and consistent with those of the empirical correlation in Figure 2F, in spite of the fact that they also appear to possess an h-propionate rather than g-propionate protein link. This suggests that the presence of the propionate at the adjacent pyrrole (f position) destabilizes the formation of the h-propionate link, possibly by preventing the necessary rotation of the heme.

A common feature of the structures of all initially formed cytochrome b_5 complexes involving hemins **1C–3C**, **5C**, and **6C** is that they all possess a propionate link to the protein matrix at either position g or position h (crystallographic 7- or 8-position). This suggests that these alternate links may be the key recognition sites in the initial encounter complex during the assembly of apocytochrome b_5 and hemin. This is in contrast to the assembly of apomyoglobin and hemin where a single propionate–protein link could be identified (La Mar et al., 1989). These alternate protein links of the g- and h-position propionates are the basis for both the unprecedented rotational heme disorder about a N–Fe–N rather than meso–Fe–meso axis observed for the monopropionate hemin **1C** and the detection of only a single and unique heme orientation for the heme with the two propionates on the same pyrrole (hemin **5C**). Current efforts are directed toward elucidating the consequences of these presently described perturbed propionate–protein contacts on redox potential.

Acknowledgments

We are indebted to F. A. Walker for useful discussions.

Supplementary Material Available

Table of absorption maxima for rat ferricytochrome reconstituted with modified hemins and figure illustrating 1D NOEs for the rat ferricytochrome b_5 reconstituted with the symmetric hemin **2C** (2 pages). Ordering information is given on any current masthead page.

References

Brunori, M., Saggese, U., Rotilio, G. C., Antonini, E., & Wyman, J. (1971) *Biochemistry 10*, 1604–1609.

Burns, P. D. (1978) Ph.D. Thesis, University of California, Davis.

Eley, C. G. S., & Moore, G. R. (1983) *Biochem. J. 215*, 11–21.

Fuhrhop, J.-H., & Smith, K. M. (1975) in *Porphyrins and Metalloporphyrins* (Smith, K. M., Ed.) p 802, Elsevier, Amsterdam.

Funk, W. D., Lo, T. P., Mauk, M. R., Brayer, G. D., MacGillivray, R. T. A., & Mauk, A. G. (1990) *Biochemistry 29*, 5500–5508.

Hartshorn, R. T., Mauk, M. R., & Moore, G. T. (1987) *FEBS Lett. 213*, 391–395.

Hauksson, J. B., La Mar, G. N., Pandey, R. K., Rezzano, I. N., & Smith, K. M. (1990) *J. Am. Chem. Soc. 112*, 8215–8224.

Hultquist, D. E., Sannes, L. G., & Juckett, D. A. (1984) *Curr. Top. Cell. Reg. 24*, 287–300.

Jameson, D. M., Gratton, E., Weber, G,. & Alpert, B. (1984) *Biophys. J. 45*, 793–803.

Keller, R. M., & Wüthrich, K. (1980) *Biochim. Biophys. Acta 621*, 204–217.

Keller, R. M., & Wüthrich, K. (1981) *Biological Magnetic Resonance* (Berliner, L. J., & Reuben, J., Eds.) pp 1–52, Plenum Press, New York.

Krishnamoorthi, R., & La Mar, G. N. (1984) *Eur. J. Biochem. 138*, 135–140.

La Mar, G. N. (1979) in *Biological Applications of Magnetic Resonance* (Shulman, R. G., Ed.) pp 305–343, Academic Press, New York.

La Mar, G. N., Burns, P. D., Jackson, J. T., Smith, K. M., Langry, K. C., & Strittmatter, P. (1981) *J. Biol. Chem. 256*, 6075–6079.

La Mar, G. N., Emerson, S. D., Lecomte, J. T. J., Pande, U., Smith, K. M., Craig, G. W., & Kehres, L. A. (1986) *J. Am. Chem. Soc 108*, 5568–5573.

La Mar, G. N., Pande, U., Hauksson, J. B., Pandey, R. K., & Smith, K. M. (1989) *J. Am. Chem. Soc. 111*, 485–489.

Lee, K. B., La Mar, G. N., Kehres, L. A., Fujinari, E. M., Smith, K. M., Pochapsky, T. C., & Sligar, S. G. (1990) *Biochemistry 29*, 9623–9631.
Livingston, D. J., McLachlan, S. J., La Mar, G. N., & Brown, W. D. (1985) *J. Biol. Chem. 260*, 15699–15707.
Mathews, F. S. (1980) *Biochim. Biophys. Acta 622*, 375–379.
Mathews, F. S., Czerwinski, E. W., & Argos, P. (1979) in *The Porphyrins* (Dolphin, D., Ed.) Vol. 7, pp 107–147, Academic, New York.
Mauk, M. R., & Mauk, A. G. (1982) *Biochemistry 21*, 1843–1846.
Mauk, M. R., & Mauk, A. G. (1986) *Biochemistry 25*, 7085–7091.
Mauk, M. R., Reid, L. S., & Mauk, A. G. (1982) *Biochemistry 21*, 1843–1846.
McLachlan, S. J., La Mar, G. N., & Sletten, E. J. (1986a) *J. Am. Chem. Soc. 108*, 1285–1291.
McLachlan, S. J., La Mar, G. N., Burns, P. D., Smith, K. M., & Langry, K. C. (1986b) *Biochim. Biophys. Acta 874*, 274–284.
McLachlan, S. J., La Mar, G. N., & Lee, K. B. (1988) *Biochim. Biophys. Acta 957*, 430–445.
Neuhaus, D., & Williamson, M. (1989) *The Nuclear Overhauser Effect*, VCH Publishers, New York.
Ozols, J., & Strittmatter, P. (1964) *J. Biol. Chem. 239*, 1018–1023.
Pandey, R. K., Rezzano, I. M., & Smith, K. M. (1987) *J. Chem. Res., Miniprint*, 2171–2192.
Reid, L. S., Taniguchi, V. T., Gray, H. B., & Mauk, A. G. (1982) *J. Am. Chem. Soc. 104*, 7516–7519.
Reid, L. S., Mauk, M. R., & Mauk, A. G. (1984) *J. Am. Chem. Soc. 106*, 2182–2185.
Reid, L. S., Lim, A. R., & Mauk, A. G. (1986) *J. Am. Chem. Soc. 108*, 8197–8201.
Rogers, K. K., Pochapsky, T. C., & Sligar, S. G. (1988) *Science 240*, 1657–1659.
Salemme, F. R. (1976) *J. Mol. Biol. 102*, 563–568.
Sandstrom, J. (1982) *Dynamic NMR Spectroscopy*, Academic Press, London.
Shulman, R. G., Glarum, S. H., & Karplus, M. (1971) *J. Mol. Biol. 57*, 93–115.
Smith, K. M., & Craig, G. W. (1983) *J. Org. Chem. 48*, 4302–4306.
Smith, K. M., Eivazi, F., & Martynenko, Z. (1981) *J. Org. Chem. 46*, 2189–2193.
Stayton, P. S., Fisher, M. T., & Sligar, S. G. (1988) *J. Biol. Chem. 263*, 13544–13548.
Strittmatter, P., Spatz, L., Corcoran, D., Rogers, M. J., Setlow, B., & Redline, R. (1974) *Proc. Natl Acad. Sci. U.S.A. 71*, 4565–4569.
Tamburini, P. P., & Schenkman, J. B. (1986) *Arch. Biochem. Biophys. 245*, 5512–5522.
Tamura, M., Asakura, T., & Yonetani, T. (1973) *Biochim. Biophys. Acta 295*, 467–479.
Teale, F. W. J. (1959) *Biochim. Biophys. Acta 35*, 543.
von Bodman, S. B., Schuler, M. A., Jollie, D. R., & Sligar, S. G. (1986) *Proc. Natl. Acad. Sci. U.S.A. 83*, 9443–9447.
Walker, F. A., Emrick, D., Rivera, J. E., Hanquet, B. J., & Buttlaire, D. H. (1988) *J. Am. Chem. Soc. 110*, 6234–6240.
Wendolosk, J. J., Matthew, J. B., Weber, P. C., & Salemme, F. R. (1987) *Science 238*, 794–797.

A Differential Scanning Calorimetric Study of the Thermal Unfolding of Seven Mutant Forms of Phage T4 Lysozyme†

Patrick Connelly, Lily Ghosaini, Cui-Qing Hu, Shinichi Kitamura, Akiyoshi Tanaka, and Julian M. Sturtevant*
Departments of Chemistry and of Molecular Biophysics and Biochemistry, Yale University, New Haven, Connecticut 06511
Received April 2, 1990; Revised Manuscript Received October 25, 1990

ABSTRACT: High-sensitivity differential scanning calorimetry has been applied to the study of the reversible thermal unfolding of the lysozyme of T4 bacteriophage in which the threonine residue at position 157 has been replaced by seven different residues. High-resolution structures derived from X-ray crystallography have been reported for these and six other mutants by Alber et al. [Alber, T., Dao-Pin, S., Wilson, K., Wozniak, J. A., Cook, S. P., & Matthews, B. W. (1987) *Nature 330*, 41–46]. At pH 2.5 the changes relative to the wild-type protein in the standard free energy of unfolding produced by these mutations indicate apparent destabilizations of 0.6 kcal mol^{-1} (T157R) to 1.9 kcal mol^{-1} (T157I), whereas the changes in enthalpy of unfolding range from −5.8 kcal mol^{-1} (T157N) to 11.9 kcal mol^{-1} (T157E). Since the denaturations are in all cases accompanied by large changes in heat capacity amounting to 2.5 kcal K^{-1} mol^{-1}, both the free energies and enthalpies are functions of temperature. An intriguing feature of the present results is the relatively large enthalpy changes and the corresponding compensating entropy changes. Our present understanding of the intramolecular energetics of proteins is insufficient to account for these changes.

The recent literature has reported studies of the effects of several single amino acid replacements in a protein on the energetics of thermal unfolding [λ repressor (Hecht et al., 1984, 1985); staphylococcal nuclease (Shortle et al., 1988; Tanaka et al., unpublished data); lysozyme of T4 phage (Alber et al., 1987; Kitamura & Sturtevant, 1989); tailspike protein of phage P22 (Sturtevant et al., 1989)]. In those studies the various replacements in a molecule were each at a different location. It was pointed out by Alber et al. (1987) that study of several different replacements at a single site in a protein might give detailed information concerning the contributions

† Generous support was received by way of Grant GM-04725 from the National Institutes of Health and Grant PCM-8417341 from the National Science Foundation.
* Author to whom correspondence should be addressed.

0006-2960/91/0430-1887$02.50/0